Observational Diagnostics of a Parametrized Deceleration Parameter in FRW Cosmology

Bhupendra Kumar Shukla , Deger Sofuoglu , Aroonkumar Beesham * , Rishi kumar Tiwari , Mfunafuthi siyabonga Msweli

Posted Date: 3 February 2026

doi: 10.20944/preprints202602.0082.v1

Keywords: parametrized decelerated parameter; radiation, matter and dark energy eras; observational constraints; current accelerated expansion of universe; analysis of parameters

Article

Observational Diagnostics of a Parametrized Deceleration Parameter in FRW Cosmology

Bhupendra Kumar Shukla [1], D. Sofuoğlu [2], A. Beesham [3,4,5,6,*], R K Tiwari [7] and Mfanafuthi Siyabonga Msweli [4]

[1] Department of Mathematics, Govt. Tilak PG College Katni 483501(M.P.)India
[2] Department of Physics, Istanbul University, Vezneciler 34134, Fatih, Istanbul, Turkey
[3] Faculty of Applied and Health Sciences, Mangosuthu University of Technology, P O Box 12363, Jacobs 4026, KwaZulu-Natal, South Africa
[4] Department of Mathematical Sciences, University of Zululand, P Bag X1001, Kwa-Dlangezwa 3886, South Africa
[5] ational Institute for Theoretical and Computational Sciences (NITheCS), South Africa
[6] DSTI-NRF Centre of Excellence in Mathematical and Statistical Sciences (CoE-MaSS), South Africa
[7] Department of Mathematics, Govt.PG Science College, Rewa 486001(M.P.)India
* Correspondence: abeesham@yahoo.com

Abstract

The evolution of the deceleration parameter $q(z)$ plays a crucial role in understanding the dynamics of dark energy within the framework of modern cosmology. In this study, we perform a parametric reconstruction of $q(z)$ in a spatially flat Friedmann–Robertson–Walker (FRW) Universe composed of radiation, pressureless dark matter, and dark energy. We consider a physically motivated form of $q(z)$ that effectively describes the transition of the Universe from a decelerating to an accelerating expansion phase. This parametrization is incorporated into the Friedmann equations to derive the corresponding Hubble parameter, which is then confronted with a comprehensive set of observational data, including Hubble parameter measurements $H(z)$, Type Ia supernovae (SNIa), and Baryon Acoustic Oscillations (BAO) data. Employing the Markov Chain Monte Carlo (MCMC) approach, we constrain the model parameters using the combined $H(z) + SNIa + BAO$ dataset. The best-fit parameters are subsequently used to reconstruct the cosmographic quantities, such as the deceleration, jerk, and snap parameters, which provide deeper insight into the expansion history of the Universe. Finally, a comparative analysis with the standard ΛCDM model is carried out to assess the compatibility and effectiveness of the proposed parametrization.

Keywords: parametrized decelerated parameter; radiation, matter and dark energy eras; observational constraints; current accelerated expansion of universe; analysis of parameters

PACS: 04.50.kd; 98.80.–k; 98.80.JK

1. Introduction

A wealth of observational evidence from various astronomical surveys strongly indicates that the Universe is currently undergoing a phase of accelerated expansion [1–3]. This unexpected and profound discovery has opened a new frontier in modern cosmology, prompting extensive theoretical and observational investigations into the fundamental mechanisms driving this expansion. The scientific community has proposed several cosmological models in response, which broadly fall into two primary categories: (i) modifications to the gravitational sector of Einstein's field equations [4,5], and (ii) the inclusion of exotic matter-energy components, most notably dark energy (DE), within the standard cosmological framework [6–8]. In this study, we focus on the latter approach, wherein dark energy is posited as the principal agent responsible for the late-time acceleration of the Universe. DE is characterized by its ability to break the criteria of the strong energy condition, thereby inducing repulsive gravitational effects that lead to the transition from an early decelerating phase to the current

 doi:10.20944/preprints202602.0082.v1

accelerating epoch [9]. An extensive spectrum of DE models has been introduced to capture this behavior, each offering distinct theoretical insights and observational signatures [10–14]. Among these, The conventional Λ Cold Dark Matter (ΛCDM) model has emerged as the most widely accepted paradigm. It assumes a cosmological constant (Λ) as the DE component with a constant equation of state $w = -1$ [15]. Despite its remarkable success in describing a large spectrum of cosmological observations, the ΛCDM model has its limitations. Notable among these are the fine-tuning problem, the coincidence problem, and the age discrepancy issue [16–18]. To overcome these conceptual challenges, alternative DE models have been proposed. This category includes scalar field models like quintessence [11], phantom fields [19,20], k-essence [21], and tachyon fields [22]. While these models provide valuable perspectives on the possible behavior of DE and the ultimate fate of the Universe, the origin and dynamics of cosmic acceleration continue to pose deep theoretical challenges and remain at the forefront of modern cosmological research.

Central to modern cosmology lies the challenge of elucidating the mechanism responsible for the Universe's late-time accelerated expansion. Among the various approaches, the phenomenological parametrization of the equation of state (EoS) parameter has garnered substantial interest for its versatility in probing cosmic acceleration without committing to a specific dark energy (DE) model [23–25]. This model-independent method involves assuming a functional form for the EoS or associated cosmological quantities and constraining the resulting parameters obtained through observational datasets. Instead of specifying the microphysical nature of DE, it seeks to describe the underlying dynamics through an assumed evolutionary behavior that best fits the data. Despite its strengths, such as minimal theoretical bias and flexibility in capturing diverse expansion histories, this parametric framework is not without limitations. Common challenges include potential divergences in certain parametrizations at high redshift, and the possibility of missing subtle dynamical features of DE due to imposed functional forms [26]. Nevertheless, parametrizations have proven effective in offering insights into the cosmological evolution and continue to contribute significantly to in model-independent diagnostics of the Universe's expansion. Inspired by these efforts, attention has also shifted toward the parametrization of the deceleration parameter $q(z)$, which directly encapsulates the acceleration history of the Universe. As a key cosmographic quantity, $q(z)$ describes the rate of change of the expansion and inherently captures the transition from the past decelerated phase—dominated by matter—to the present accelerated phase driven by DE. The sign of q serves as an indicator of the expansion regime, with $q > 0$ signifying deceleration and $q < 0$ indicating acceleration. Therefore, reconstructing $q(z)$ from observational data offers an intuitive and insightful way to trace the cosmic expansion history and to assess the consistency of cosmological models with observed phenomena [27–29].

In recent years, a variety of theoretical approaches have been developed to explore the dynamical history of the Universe through the parametrization of the deceleration parameter $q(z)$ as a function of cosmic time t, scale factor $a(t)$, or redshift z [30–39]. These parametrizations offer a phenomenologically appealing and model-independent route to investigate the expansion dynamics without committing to a specific gravitational framework or DE model.Such techniques provide finite and tractable solutions, allowing for a detailed analysis of cosmic expansion and the transition from decelerated to accelerated phases. However, these methods also share certain limitations inherent to parametric schemes. Chief among them is the dependence on an assumed functional form, which may overlook or oversimplify subtle physical aspects of the cosmic evolution. Moreover, the absence of a unique or universally accepted theoretical model for the entire expansion history introduces ambiguity into the interpretation of such parametrizations. Consequently, while the use of $q(z)$ parametrizations presents a valuable preliminary tool for understanding the Universe's accelerated expansion, it is often viewed as an intermediate step toward more complete theoretical or observational frameworks.

A central objective of the present work is to tightly set constraints on the free parameters of the proposed cosmological model using a combination of recent observational datasets. In particular, we utilize the latest compilation of 31 Hubble parameter $H(z)$ observations collected via cosmic chronometers, the Pantheon+ sample comprising 1701 Type Ia supernovae (SNIa) data points, and 26

 doi:10.20944/preprints202602.0082.v1

Baryon Acoustic Oscillation (BAO) measurements. These diverse and complementary datasets provide a robust foundation for examining the viability of the model across different cosmological epochs. To extract the best-fit values of the model parameters, Statistical analysis is implemented using the Markov Chain Monte Carlo (MCMC) technique. This approach allows for an efficient exploration of the set of parameters and offers precise constraints consistent with the latest observations. The model is further tested using a joint likelihood analysis via a standard χ^2-minimization procedure, applied to the combined dataset $H(z) + \text{SNIa} + \text{BAO}$, thereby ensuring a comprehensive comparison with observational evidence [38,40–43].

The structure of this paper is organized as follows: In Section II, we present the basic equations governing the Friedmann–Robertson–Walker (FRW) framework. Section III introduces the chosen parameterization of the deceleration parameter $q(z)$ and outlines its physical motivation. Section IV describes the methodology and statistical analysis based on the MCMC approach used for parameter estimation from observational datasets. In Section V, the cosmographic parameters are computed and analyzed to explore the kinematic behavior of the model. Section VI discusses the relation between the equation of state parameter and the deceleration parameter. The main results and their implications are presented and discussed in Section VII. Finally, Section VIII summarizes the conclusions and highlights possible directions for future research.

2. Basic Equations of the FRW Model

We adopt the FRW metric to describe a spatially flat, homogeneous, and isotropic Universe. The line element in spherical coordinates is given by

$$ds^2 = -dt^2 + a^2(t)\left[dr^2 + r^2\left(d\theta^2 + \sin^2\theta\, d\phi^2\right)\right], \tag{1}$$

where $a(t)$ is the scale factor that characterizes the expansion of the Universe as a function of cosmic time t.

The energy-momentum tensor for a perfect fluid, which serves as the source in Einstein's field equations, is written as

$$T_{\mu\nu} = (\rho + p)u_\mu u_\nu + p g_{\mu\nu}, \tag{2}$$

where ρ is the energy density, p is the pressure, and u^μ is the four-velocity of the fluid, normalized such that $u^\mu u_\mu = -1$.

The Einstein field equations, when applied to the FRW metric, simplify to the Friedmann equations that describe the Universe's dynamics:

$$H^2 = \frac{8\pi G}{3}\rho, \tag{3}$$

$$\frac{\ddot{a}}{a} = -\frac{4\pi G}{3}(\rho + 3p), \tag{4}$$

where $H = \dot{a}/a$ is the Hubble parameter, and over-dots represent time derivatives. Note that Equation (4) can equivalently be written using the continuity equation as $\dot{H} = -4\pi G(\rho + p)$.

Assuming independent conservation for each component (radiation r, matter m, dark energy d), the energy conservation equations are:

$$\dot{\rho}_r + 3H(\rho_r + p_r) = 0, \tag{5}$$

$$\dot{\rho}_m + 3H(\rho_m + p_m) = 0, \tag{6}$$

$$\dot{\rho}_d + 3H(\rho_d + p_d) = 0. \tag{7}$$

Standard integration yields the evolution for radiation ($p_r = \rho_r/3$) and pressureless matter ($p_m = 0$) as:

$$\rho_r = \rho_{r0}(1+z)^4, \quad \rho_m = \rho_{m0}(1+z)^3, \tag{8}$$

 doi:10.20944/preprints202602.0082.v1

where ρ_{i0} denotes the present-day density of component i and $1+z = a_0/a$.

We define the deceleration parameter as

$$q(z) = -1 + \frac{(1+z)}{H(z)}\frac{dH}{dz}. \tag{9}$$

This parameter measures the acceleration of the Universe's expansion. By integrating Equation (9), we obtain the kinematic evolution of the Hubble parameter solely in terms of the deceleration parameter:

$$H(z) = H_0 \exp\left[\int_0^z \frac{1+q(z')}{1+z'}dz'\right]. \tag{10}$$

We define the normalized Hubble parameter as $E(z) = H(z)/H_0$.

Assuming a flat universe ($\Omega_k = 0$) containing radiation, pressureless matter, and a dark energy component, the Friedmann equation relates the Hubble parameter to the density parameters as:

$$E^2(z) = \Omega_{r0}(1+z)^4 + \Omega_{m0}(1+z)^3 + \Omega_{DE}(z). \tag{11}$$

The corresponding dimensionless density parameters at the current epoch are given by $\Omega_{i0} = 8\pi G\rho_{i0}/(3H_0^2)$.

By rearranging Equation (11), we can isolate the dimensionless dark energy density parameter, $\Omega_{DE}(z)$, in terms of the kinematic Hubble rate derived from our ansatz. This yields the reconstruction equation:

$$\Omega_{DE}(z) = E^2(z) - \Omega_{m0}(1+z)^3 - \Omega_{r0}(1+z)^4, \tag{12}$$

where $E(z)$ is obtained from Equation (10).

It is important to emphasize the philosophy of this approach: we do not assume a specific theoretical model for dark energy (such as a cosmological constant) a priori. Instead, $\Omega_{DE}(z)$ is treated as a derived quantity. Its evolution is determined dynamically by the reconstructed history of $q(z)$ and the value of Ω_{m0}. This approach guarantees total consistency with the standard Friedmann equations. Instead of imposing a form for ρ_d to solve for $H(z)$, we use the kinematically derived $H(z)$ to solve for the required evolution of $\rho_d(z)$.

Using the derived $\Omega_{DE}(z)$, we can further reconstruct the effective dark energy equation of state parameter, $w_{DE}(z)$:

$$w_{DE}(z) = \frac{\frac{2q(z)-1}{3} - \frac{1}{3}\frac{\Omega_{r0}(1+z)^4}{E^2(z)}}{1 - \frac{\Omega_{m0}(1+z)^3}{E^2(z)} - \frac{\Omega_{r0}(1+z)^4}{E^2(z)}}. \tag{13}$$

Regarding the radiation component, we fix Ω_{r0} based on the standard photon and neutrino background temperatures (typically $\Omega_{r0} \approx 2.47 \times 10^{-5} h^{-2}$ for photons plus standard neutrinos). The present-day dark energy density Ω_{d0} is then constrained by the flatness condition at $z = 0$:

$$\Omega_{d0} = 1 - \Omega_{m0} - \Omega_{r0}. \tag{14}$$

Thus, our free parameters in the MCMC analysis are the coefficients of the $q(z)$ parametrization, Ω_{m0}, and H_0.

We have derived the basic equations governing a spatially flat FRW Universe filled with radiation, dark matter, and dark energy. We presented the Friedmann equations, conservation equations, and expressions for the deceleration parameter. The evolution of each component's energy density is specified, and the general form of the Hubble parameter $H(z)$ as a function of redshift is established. These equations serve as the fundamental framework for studying the dynamics and late-time evolution of the Universe.

 doi:10.20944/preprints202602.0082.v1

3. Parameterization of the Deceleration Parameter $q(z)$ and Its Motivation

Thermodynamics plays a fundamental role in modern cosmology, especially in understanding the large-scale evolution of the universe and its compatibility with the basic laws of physics. A key principle in this context is the second law of thermodynamics, which states that the entropy S of an isolated system cannot decrease with time, i.e.

$$dS \geq 0,$$

and that, as the system evolves toward thermodynamic equilibrium, the entropy approaches a maximum value, implying concavity of the entropy functional,

$$d^2S < 0,$$

during the late-time evolution [44]. Although originally formulated for ordinary thermodynamic systems, these principles naturally extend to the universe when treated as a thermodynamic entity.

In the Friedmann–Robertson–Walker (FRW) cosmological framework, the entropy of the cosmic fluid becomes closely linked to the entropy associated with the causal horizon, which is most suitably identified with the apparent horizon [45]. The radius of the apparent horizon in FRW spacetime is

$$\tilde{r}_A = \frac{1}{\sqrt{H^2 + \frac{k}{a^2}}}, \tag{15}$$

where $k = 0, +1, -1$ refers to spatially flat, closed, and open geometries, respectively [46]. Numerous studies have shown that the apparent horizon is the appropriate surface for thermodynamic analysis, as it satisfies the unified first law of thermodynamics and connects directly to gravitational field equations [47].

Neglecting quantum corrections, the entropy associated with the apparent horizon is proportional to its area,

$$A = 4\pi\tilde{r}_A^2,$$

so that for a flat FRW universe ($k = 0$), where $\tilde{r}_A = H^{-1}$, the area becomes

$$A = 4\pi H^{-2}.$$

Thus the horizon entropy satisfies

$$S_A \propto H^{-2}.$$

The second law of thermodynamics requires the horizon area to be non-decreasing and eventually concave, i.e.

$$A' = \frac{dA}{da} \geq 0, \qquad A'' = \frac{d^2A}{da^2} \leq 0,$$

ensuring the thermodynamic viability of cosmic evolution [48].

Differentiating $A = 4\pi H^{-2}$ with respect to the scale factor,

$$A' = -8\pi H^{-3}\frac{dH}{da}.$$

Using

$$z = \frac{1}{a} - 1, \qquad \frac{dz}{da} = -\frac{1}{a^2},$$

and applying the chain rule,

$$\frac{dH}{da} = \frac{dH}{dz}\frac{dz}{da},$$

 doi:10.20944/preprints202602.0082.v1

we obtain

$$A' = 8\pi \frac{1}{H^3 a^2} \frac{dH}{dz}.$$

To express dH/dz in terms of the deceleration parameter, we start from the definition

$$q = -1 - \frac{\dot{H}}{H^2},$$

and use the redshift–time relation

$$\frac{dz}{dt} = -(1+z)H, \qquad \frac{dt}{dz} = -\frac{1}{H(1+z)}.$$

This yields

$$\frac{dH}{dz} = \dot{H}\frac{dt}{dz} = -H^2(1+q)\left(-\frac{1}{H(1+z)}\right) = \frac{H(1+q)}{1+z}.$$

Since $1/(1+z) = a$, we also have

$$\frac{dH}{da} = -\frac{H(1+q)}{a}.$$

Substituting into A' gives

$$A' = \frac{8\pi(1+q)}{aH^2} = 2A\frac{1+q}{a}.$$

Thus the condition $A' \geq 0$ immediately implies

$$q \geq -1.$$

Differentiating A' once more,

$$A'' = \frac{d}{da}\left(2A\frac{1+q}{a}\right) = 2A'\frac{1+q}{a} + 2A\left(\frac{dq/da}{a} - \frac{1+q}{a^2}\right),$$

which simplifies to

$$A'' = 2A\left[\frac{(1+q)(1+2q)}{a^2} + \frac{dq}{da}a^{-1}\right].$$

At late times ($a \to \infty$) the term proportional to a^{-2} decays, so the dominant contribution becomes

$$A'' \simeq 2A\,\frac{dq/da}{a}.$$

Requiring $A'' \leq 0$ leads to

$$\frac{dq}{da} < 0.$$

Since $dz/da = -1/a^2 < 0$, this condition is equivalent to

$$\frac{dq}{dz} > 0 \qquad (z \to -1).$$

Therefore the deceleration parameter must approach the de Sitter value $q \to -1$ monotonically from above in the far future, ensuring that the apparent-horizon entropy is maximized.

Motivated by these thermodynamic considerations, we adopt the phenomenological parametrization proposed by Xu et al. [49]:

$$q(z) = q_0 + \frac{q_1 z}{1+z}, \tag{16}$$

where q_0 denotes the present value of the deceleration parameter (i.e., at $z = 0$), and q_1 characterizes the rate of evolution of $q(z)$ with redshift. This parameterization possesses several desirable properties:

 doi:10.20944/preprints202602.0082.v1

- At present time ($z = 0$), the deceleration parameter reduces to $q(0) = q_0$.
- At high redshift ($z \gg 1$), it asymptotically approaches $q(z) \to q_0 + q_1$, which can be interpreted as the deceleration value in the matter-dominated era.
- The functional form ensures a smooth transition between the early- and late-time cosmic evolution.
- It avoids divergences at both low and high redshifts and provides good agreement with observational data.

Thus, the parameterization in Equation (16) offers a simple yet powerful tool to investigate the dynamics of the Universe and analyze observational constraints on cosmic acceleration. In order to obtain the expansion history consistent with the above deceleration dynamics and thermodynamic requirements, we integrate the kinematical relation between $q(z)$ and $H(z)$,

$$\frac{d\ln H}{dz} = \frac{1+q(z)}{1+z},$$

with the parametrization (16), we obtain the following Hubble parameter

$$H(z) = H_0(1+z)^{1+q_0+q_1}\exp\left(-\frac{q_1 z}{1+z}\right). \tag{17}$$

and in terms of the density parameters, it can be written as

$$H^2(z) = H_0^2\left[\Omega_{r0}(1+z)^4 + \Omega_{m0}(1+z)^3 + \Omega_{d0}(1+z)^{2(1+q_0+q_1)}\exp\left(-\frac{2q_1 z}{1+z}\right)\right]. \tag{18}$$

This last equation is Equation (**??**), which is specialized for our model. Here, Ω_{r0} is fixed by spatial flatness once Ω_{m0} and Ω_{d0} are specified through Equation (14) and it does not enter as an independent fitting parameter in the observational analysis.

In summary, the cosmological model employed here is purely kinematical: the total expansion history is determined by the phenomenological deceleration parameter $q(z)$, and the Hubble function $H(z)$ is derived directly from it through the relation $d\ln H/dz = (1+q)/(1+z)$. The radiation–matter–dark energy decomposition of $H^2(z)$ is used only as an observationally relevant split of the total expansion rate, without attributing any separate dynamics to individual components.

4. Parameter Estimation via MCMC Method

In modern cosmology, the accurate estimation of model parameters plays a critical role in understanding the Universe's expansion history. A Bayesian framework is often employed to extract constraints on cosmological parameters from observational data. According to Bayes' theorem, the posterior probability distribution of a parameter set θ given data D is expressed as:

$$P(\theta \mid D) = \frac{L(D \mid \theta)P(\theta)}{P(D)}, \tag{19}$$

where $P(\theta)$ is the prior distribution incorporating previous knowledge, $L(D \mid \theta)$ corresponds to the likelihood of observing the data under the model, and $P(D)$ is the evidence or normalization factor.

To efficiently sample from the posterior distribution in a high-dimensional parameter space, we apply the Markov Chain Monte Carlo (MCMC) approach through the `emcee` package [50], which implements the affine-invariant ensemble sampler. Convergence diagnostics are verified using autocorrelation analysis and visual inspection. The `GetDist` package [51] is carried out to generate the marginalized distributions and confidence contours.

Our analysis constrains the parameters of a cosmological model with a variable deceleration parameter using three observational datasets:

- Cosmic Chronometers (CC)
- Type Ia Supernovae (SNIa) from the Pantheon+ compilation

 doi:10.20944/preprints202602.0082.v1

- Baryon Acoustic Oscillations (BAO)

4.1. Cosmic Chronometers (CC)

Using Cosmic Chronometers, the Hubble parameter $H(z)$ can be estimated in a model-independent way through the differential aging of passively evolving galaxies. The underlying relation is given by:

$$H(z) \approx -\frac{1}{1+z}\frac{\Delta z}{\Delta t}. \tag{20}$$

We utilize 31 CC data covering the redshift interval $0.07 \lesssim z \lesssim 1.97$, compiled from Refs. [52–57]. The chi-square statistic corresponding to the CC data is given by:

$$\chi^2_{\rm CC}(\theta) = \Delta H^T(z)\, C^{-1}\, \Delta H(z), \tag{21}$$

where $\Delta H(z) = H_{\rm model}(z) - H_{\rm data}(z)$, and C is the associated covariance matrix.

4.2. Type Ia Supernovae (SNIa)

The Pantheon+ sample contains 1701 SNe Ia from 1550 unique events over the redshift range $0 \leq z \leq 2.3$ [58]. The observed distance modulus is defined as

$$\mu_{\rm obs}(z) = m(z) - M_{\rm abs}, \tag{22}$$

where $m(z)$ is the apparent magnitude and $M_{\rm abs}$ denotes the intrinsic absolute magnitude of SNe Ia. The theoretical distance modulus is modeled as

$$\mu_{\rm model}(z,\theta) = 5\log_{10}\left[\frac{d_L(z)}{\rm Mpc}\right] + \mathcal{M}, \tag{23}$$

where $\mathcal{M}$ is treated as a nuisance parameter that absorbs the degeneracy between $M_{\rm abs}$ and the Hubble constant, and it is sampled together with the cosmological parameters in the MCMC analysis.

In a spatially flat universe, the luminosity distance is written as

$$d_L(z) = \frac{1+z}{H_0}\int_0^z \frac{dz'}{E(z')}. \tag{24}$$

The chi-squared function is then constructed as

$$\chi^2_{\rm SNIa} = \Delta\mu^T C_{\rm t}^{-1} \Delta\mu, \tag{25}$$

with $C_{\rm t} = C_{\rm stat} + C_{\rm sys}$, and

$$\Delta\mu = \mu_{\rm obs}(z_i) - \mu_{\rm model}(z_i,\theta). \tag{26}$$

4.3. Baryon Acoustic Oscillations (BAO)

BAO observations provide geometric measurements of the large-scale structure through the sound horizon scale r_d, defined at the drag epoch $z_d \approx 1060$:

$$r_d = \int_{z_d}^{\infty} \frac{c_s(z)}{H(z)}\, dz, \tag{27}$$

where $c_s(z)$ denotes the sound speed in the early Universe. This expression is shown only to indicate the physical meaning of r_d; it is not used in the likelihood analysis, since r_d is treated as a free nuisance parameter sampled together with the cosmological parameters [59–62].

 doi:10.20944/preprints202602.0082.v1

We incorporate BAO data from SDSS-IV and DESI Year 1 [62,63], which constrain:

$$D_H(z) = \frac{c}{H(z)}, \tag{28}$$

$$D_M(z) = \frac{c}{H_0}\int_0^z \frac{dz'}{E(z')}, \tag{29}$$

$$D_V(z) = \left[zD_M^2(z)D_H(z)\right]^{1/3}. \tag{30}$$

The chi-square statistic corresponding to the BAO data is expressed as:

$$\chi^2_{D_X/r_d} = \Delta D_X^T\, C_{D_X}^{-1}\, \Delta D_X, \tag{31}$$

with

$$\Delta D_X = \frac{D_{X,\mathrm{model}}(z)}{r_d} - \frac{D_{X,\mathrm{data}}(z)}{r_d}, \tag{32}$$

and $C_{D_X}^{-1}$ is the inverse covariance matrix.

4.4. Results and Posterior Distributions

Using the combined `CC+SNIa+BAO` dataset, we perform a comprehensive MCMC analysis of the model constructed through the parametrization (16). The resulting corner plot (Figure 1) displays the posterior distributions along with the 1σ and 2σ credible intervals. The best-fit values, prior ranges, and uncertainties are summarized in Table 1.

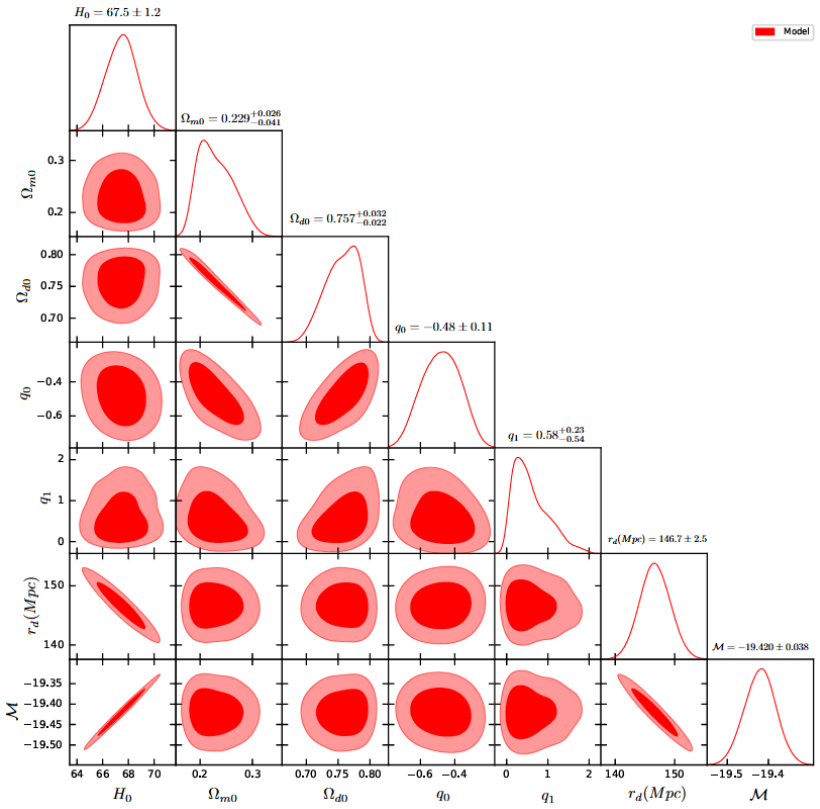

Figure 1. Posterior probability distributions and corresponding 1σ, 2σ confidence contours for the model parameters from the combined datasets.

 doi:10.20944/preprints202602.0082.v1

Table 1. The best-fit values for the model parameters obtained using the combined CC, SNIa, and BAO datasets.

MCMC Results			
Model	Parameter	Prior Range	Best-fit Value
ΛCDM Model	H_0	[50,100]	68.3 ± 0.9
	Ω_{m0}	[0,1]	0.300 ± 0.015
	Ω_{d0}	[0,1]	0.700 ± 0.015
	r_d (Mpc)	[100,200]	147.1 ± 0.3
Model	H_0	[50, 100]	67.5 ± 1.2
	Ω_{m0}	[0,1]	$0.229^{+0.026}_{-0.041}$
	Ω_{d0}	[0,1]	$0.757^{+0.032}_{-0.022}$
	q_0	$[-0.7,-0.25]$	-0.48 ± 0.11
	q_1	[0, 2]	$0.58^{+0.23}_{-0.54}$
	$\mathcal{M}$	$[-20,-18]$	-19.420 ± 0.038
	r_d (Mpc)	[100,200]	146.7 ± 2.5

4.5. Model Comparison with ΛCDM

To evaluate the model's performance, we compare its predictions with those of the ΛCDM model. Figures 2 and 3 show that the Hubble parameter and distance modulus curves for our model align well with observations.

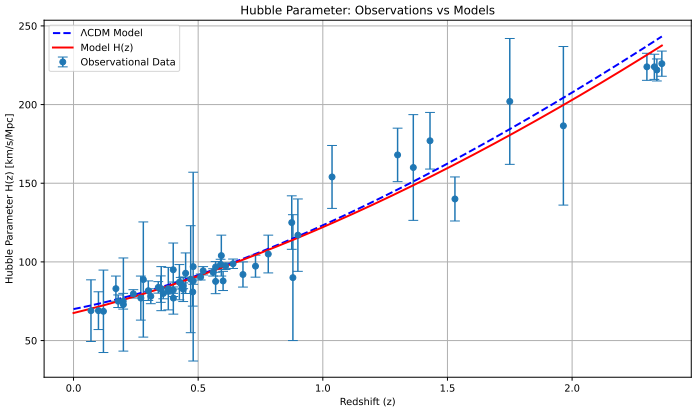

Figure 2. Comparison of the Hubble parameter curve predicted by the model with that of the ΛCDM model.

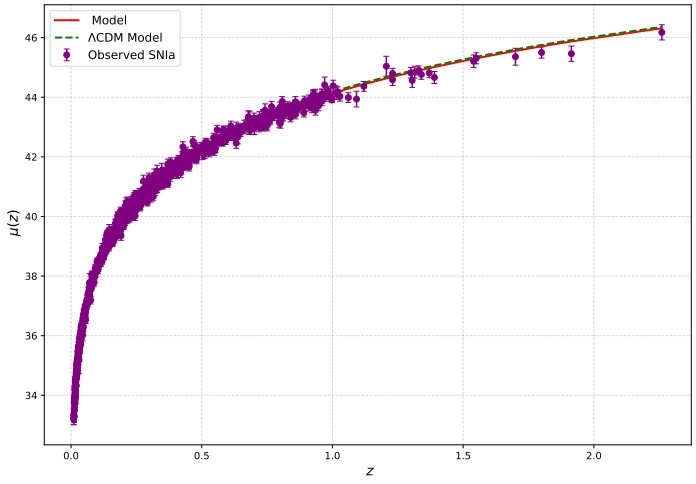

Figure 3. Comparison of the distance modulus curve between the model and ΛCDM model.

 doi:10.20944/preprints202602.0082.v1

5. Cosmographic Parameters

A model-independent analysis of the Universe's kinematics is achieved through cosmography by expressing the scale factor as a Taylor series in cosmic time. The deceleration, jerk, and snap parameters, essential in cosmography, come from the scale factor's higher-order derivatives and allow us to investigate the expansion history of the Universe without explicitly assuming any underlying dynamics or DE model.

5.1. Deceleration Parameter

The deceleration parameter $q(z)$ is essential for understanding whether the cosmic expansion is accelerating or slowing down. It is given as:

$$q = -\frac{\ddot{a}}{aH^2}, \tag{33}$$

where a is the scale factor and $H = \dot{a}/a$ is the Hubble parameter. A negative value of q indicates accelerated expansion.

Figure 4 presents the evolution of $q(z)$ along with the corresponding 1σ confidence region derived from MCMC analysis. The deceleration parameter smoothly transitions from positive to negative values at the redshift $z_{\rm tr} = 0.69^{+0.06}_{-0.11}$, marking the epoch when the Universe shifted from decelerated expansion (dominated by matter) to accelerated expansion (dominated by DE). The present-day value is found to be $q_0 = -0.48 \pm 0.11$, which aligns well with ΛCDM predictions (e.g., $q_0 \approx -0.55$, $z_{\rm tr} \approx 0.67$) based on the Planck 2018 results.

At high redshifts ($z \to \infty$), the deceleration parameter approaches $q(z \to \infty) = q_0 + q_1$, as expected for standard matter-dominated scenarios. Notably, the values of q_0 and $z_{\rm tr}$ show slight deviations from the ΛCDM model depending on the dataset used. These discrepancies might be linked to the ongoing Hubble tension problem, a topic of considerable debate in current cosmological research.

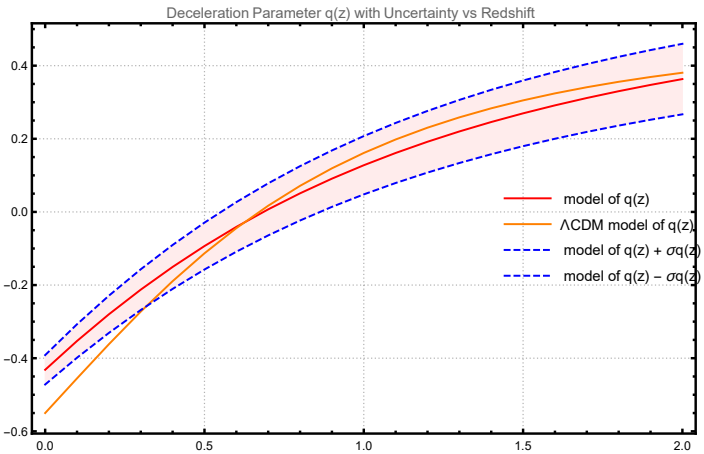

Figure 4. Evolution of the deceleration parameter $q(z)$ with 1σ error bounds.

5.2. Jerk Parameter

The jerk parameter $j(z)$ is the third derivative of the scale factor and provides information about departures from the ΛCDM model. It is defined as:

$$j = \frac{\dddot{a}}{aH^3}. \tag{34}$$

In the ΛCDM scenario, the jerk parameter is constant with value $j = 1$. Thus, deviations of $j(z)$ from unity can indicate the presence of dynamical DE or modifications to general relativity.

The evolution of $j(z)$ is plotted in Figure 5. Our analysis shows that in the early Universe, the jerk parameter significantly deviated from the standard ΛCDM value. The current value is found to

 doi:10.20944/preprints202602.0082.v1

be $j_0 \approx 0.75$, which suggests a deviation from the canonical cosmological constant. Moreover, $j(z)$ increases with time, indicating evolving cosmic acceleration behavior and a possible departure from standard cosmology.

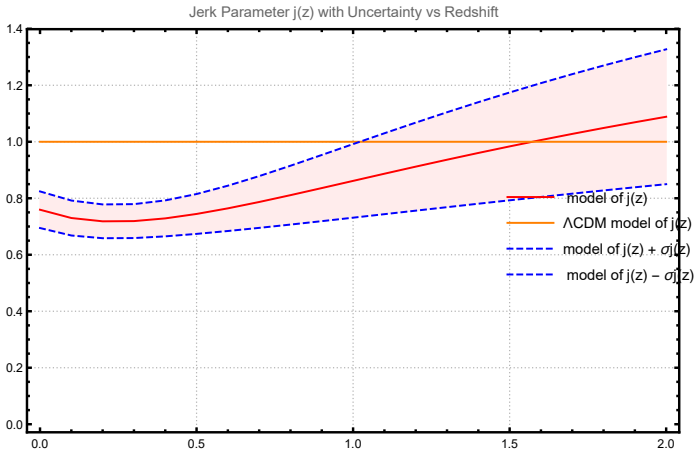

Figure 5. Evolution of the jerk parameter $j(z)$ with 1σ error bounds.

5.3. Snap Parameter

The snap parameter $s(z)$ is the fourth derivative of the scale factor and helps capture higher-order corrections to the expansion rate. It is defined as:

$$s = \frac{\dddot{a}}{aH^4}. \tag{35}$$

While less commonly used than q and j, the snap parameter is essential for detecting subtle deviations from ΛCDM, especially in models involving time-varying DE or higher-order gravity.

Figure 6 shows the redshift evolution of the snap parameter. Our model predicts a behavior for $s(z)$ that remains broadly consistent with the ΛCDM model at low redshifts, though deviations at earlier epochs may provide clues about more complex cosmological dynamics.

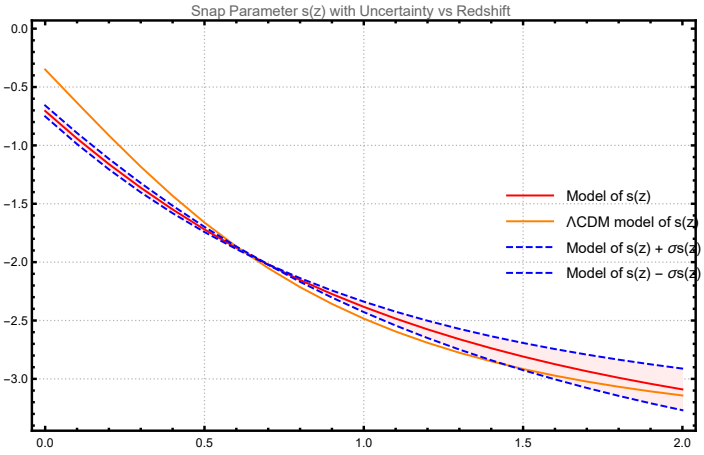

Figure 6. Evolution of the snap parameter $s(z)$ with 1σ error bounds.

6. Equation of State Parameter in General Relativity and Its Relation to Deceleration Parameter

In the framework of General Relativity, the large-scale structure and dynamics of the universe are governed by the Einstein field equations. Assuming a spatially homogeneous and isotropic FRW metric, the field equations reduce to the Friedmann equations, which govern the expansion rate of the universe through the Hubble parameter $H(z)$.

 doi:10.20944/preprints202602.0082.v1

The Equation of State (EoS) parameter of the cosmic fluid is defined as

$$w(z) = \frac{p(z)}{\rho(z)}, \tag{36}$$

where $p(z)$ and $\rho(z)$ are the total pressure and energy density of the cosmic fluid, respectively. In a universe dominated by DE and pressureless matter, this parameter plays a crucial role in determining the expansion dynamics.

Using the Friedmann equations, and assuming a perfect fluid with total density ρ and pressure p, the deceleration parameter can be related to the EoS parameter as:

$$q(z) = \frac{1}{2}[1 + 3w(z)(1 - \Omega_m(z))], \tag{37}$$

for a flat universe ($\Omega_k = 0$), where $\Omega_m(z)$ is the matter density parameter at redshift z.

Conversely, one can express $w(z)$ in terms of $q(z)$ and $\Omega_m(z)$ as:

$$w(z) = \frac{2q(z) - 1}{3[1 - \Omega_m(z)]}. \tag{38}$$

This relation allows one to reconstruct the effective equation of state parameter directly from the deceleration parameter and the matter density evolution.

Comparison with ΛCDM Model

In the context of the ΛCDM model, DE corresponds to the cosmological constant Λ, with a constant EoS parameter

$$w_\Lambda = -1. \tag{39}$$

Substituting this into Eq. (37) gives:

$$q(z) = \frac{1}{2}[1 - 3(1 - \Omega_m(z))] = \frac{3}{2}\Omega_m(z) - 1. \tag{40}$$

At the present epoch ($z = 0$), assuming $\Omega_{m0} \approx 0.3$, the deceleration parameter becomes $q_0 \approx -0.55$, indicating accelerated expansion.

In contrast, in dynamical DE models where $w(z)$ varies with time, the deceleration parameter evolves differently, allowing these models to be observationally distinguished from ΛCDM.

Physical Interpretation

The parameter $w(z)$, defined as the ratio of pressure to energy density, determines the behavior of the Universe's dominant component. Common values are:

- $w = 0$: matter,
- $w = 1/3$: radiation,
- $w = -1$: vacuum energy (cosmological constant),
- $w < -1$: phantom,
- $-1 < w < -1/3$: quintessence.

An accelerating Universe requires $w < -1/3$. In the standard ΛCDM model, as mentioned above, dark energy is represented by a cosmological constant with $w = -1$, while alternative scenarios consider redshift-dependent $w(z)$.

 doi:10.20944/preprints202602.0082.v1

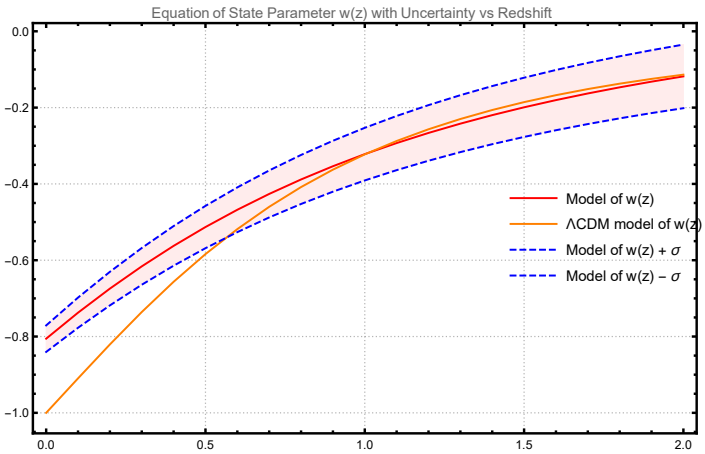

Figure 7. Evolution of the $\omega(z)$ parameter with 1σ error bounds.

Thus, precise reconstruction of $w(z)$ through observations of $q(z)$ and $H(z)$ is fundamental to understanding the nature of dark energy and testing the validity of the ΛCDM paradigm.

As illustrated in Figure 7, the evolution of the EoS parameter $\omega(z)$ with its 1σ uncertainty band further supports the consistency of our results with the ΛCDM paradigm while allowing possible deviations.

7. Results and Discussion

- **Confidence levels:** To estimate the model parameters and assess their uncertainties, we employed the Markov Chain Monte Carlo (MCMC) technique using the combined observational datasets, including cosmic chronometers $H(z)$, SNIa and baryon acoustic BAO. This comprehensive dataset combination ensures a more stringent constraint on the parameters by covering a wide redshift range and various cosmological probes. The resulting posterior distributions for the model parameters q_0,and q_1 are illustrated in Figure 1. These distributions provide insight into the most probable values of the parameters and their correlations. The marginalized one-dimensional (1D) histograms represent the probability distributions for each individual parameter, while the two-dimensional (2D) confidence contours illustrate the covariances between the parameter pairs. The 2D contour plots are drawn at 68% (1σ) and 95% (2σ) confidence levels, representing the regions within which the true values of the parameters are likely to lie, assuming Gaussian errors. The best-fit values and corresponding credible intervals are summarized in Table 1. The results confirm that the proposed parametrization is capable of fitting the combined data well, with parameter constraints that are both tight and consistent across the datasets. The posterior analysis also shows a clear preference for a late-time accelerating universe, as indicated by the negative values of the present deceleration parameter q_0. Overall, the joint posterior distributions and confidence contours provide a strong statistical foundation for evaluating the viability and physical implications of the proposed deceleration parameter model.
- The deceleration parameter $q(z)$, which provides information about the acceleration or deceleration of the Universe's expansion, is shown in Figure 4. We find that $q(z)$ lies well within the 1σ confidence interval of the ΛCDM model throughout the redshift range considered. The transition redshift—defined as the redshift $z_{\rm tr}$ at which the Universe transitioned from decelerated to accelerated expansion—is found to be approximately $z_{\rm tr} \approx 0.65$. This value is very close to that predicted by the ΛCDM model, which gives $z_{\rm tr} \approx 0.67$. Similarly, the present-day value of the deceleration parameter is $q_0 \approx -0.48$, which also aligns well with the ΛCDM prediction of $q_0 \approx -0.55$.

  To assess the efficacy and physical motivation behind our choice of deceleration parameter form (Eq. 16), it is instructive to compare it with other parametrizations proposed in the literature.

 doi:10.20944/preprints202602.0082.v1

Several different functional forms for $q(z)$ have been comprehensively reviewed by Pacif et al. [64]. Among these, we consider the forms most comparable to our own. Nair et al. [65] explored three different parametrizations:

$$q_I(z) = q_0 + q_1 z,$$
$$q_{II}(z) = q_2 + \frac{q_3 z}{1+z},$$
$$q_{III}(z) = q_4 + \frac{q_5 z}{(1+z)^2}.$$

However, it was found that none of these forms provided a satisfactory fit to the observational data when multiple datasets were considered simultaneously. This shortcoming further motivates our choice of a more viable and observationally consistent form, given by Eq. 16.

Our model strikes a balance between simplicity and empirical accuracy. It introduces just enough flexibility to capture the dynamics of cosmic acceleration without overfitting the data. Importantly, adding more than two free parameters to $q(z)$ often renders the model computationally intensive and analytically intractable, without a significant improvement in fit quality.

A similar form to our parametrization was proposed by Lu et al. [66], but their analysis was based only on 557 SNIa Union2 data points and 15 $H(z)$ measurements. Consequently, their model predictions did not align well with current observations.

Mamon and Das [67] introduced a slightly more complex form:$q(z) = q_0 + q_1 \frac{z(1+z)}{1+z^2}$, which offers a good phenomenological description of cosmic evolution. Likewise, del Campo et al. [68] and Pavón et al. [69] considered the form: $q(z) = -1 + \frac{3}{2} \cdot \frac{(1+z)^{q_2}}{q_1+(1+z)^{q_2}}$, a more intricate expression requiring numerical integration to compute $H(z)$. Due to its complexity, we do not elaborate further on additional parametrizations studied in their work. Xu et al. [49] proposed a logarithmic form: $q(z) = a + \frac{b}{1+\ln(1+z)}$, which provided reasonable constraints with observational data. However, the derived transition redshift $z_t = 0.54$ is notably lower than the ΛCDM prediction, suggesting limitations in capturing the late-time acceleration dynamics accurately.

Another complex form, $q(z) = a + b\left(-d + \frac{\ln(N+z)}{1+z}\right)$, was investigated by Mamon and Das [70], involving four model parameters (a, b, d, and N). While flexible, this model introduces unnecessary complexity and lacks clear physical interpretability [70].

More recently, Myrzakulov et al. [71] proposed a simple yet effective parametrization: $q(z) = q_1 - \frac{q_1+1}{(1+z)^{q_2}+1}$, which performs well against observational data. However, their best-fit value for the present-day deceleration parameter is $q_0 = -0.362 \pm 0.032$, which deviates significantly from the ΛCDM value. In contrast, our model's prediction of $q_0 \approx -0.48$ is in much better agreement, reinforcing the reliability and effectiveness of our chosen parametrization.

We now elucidate upon some other very important references that have been undertaken relating to dark energy. In the study [72], the authors investigated a cosmologically compatible model of the universe using holographic dark energy and the generalized Chaplygin-Jacobi gas framework. It was assumed that dark energy sources can be described as generalized Chaplygin-Jacobi gas, associating the Hubble horizon with the Chaplygin scalar field and incorporating specific elliptic identities. The findings suggested that the constraints align well with current observational data. Azhar et al. [73] explored the five-dimensional Einstein-Chern-Simons gravity in the context of a flat FRW universe. This framework, derived by incorporating higher-dimensional topological invariants and gauge symmetries, serves as a compelling extension of general relativity. They employed the holographic dark energy model, using the Hubble horizon as the infrared cutoff, to investigate its cosmological implications. Various choices of the interaction term Q were chosen to analyse the key cosmological parameters. The findings of this research exhibited excellent agreement with recent observational data. In the paper[74], Jawad et al. used the cosmographic approach to discuss Friedmann space-time in the presence of torsion. For this, they explored

 doi:10.20944/preprints202602.0082.v1

equations of motion that explain creation in an isotropic and homogeneous cosmic backdrop with nonzero torsion. The energy density of the holographic dark energy model was taken to depend upon the redshift parameter the reduced Planck mass and the holographic length scale. Employing certain other assumptions, consistent results for specific choices of constant parameters were obtained in the underlying scenario. Jawad et al. [75] studied the cosmic aspects of the evolving universe by taking into account mimetic gravity. They considered three well-known equation of state parameterizations in terms of the redshift function. Considering the observational values of parameters in parametrization models, they got some useful results for the underlying scenario. Additionally a numerical reconstruction of the potential as a function of the mimetic scalar field was attempted. The authors Sarnia et al. [76] investigated the cosmological and thermodynamic aspects of the Brans–Dicke theory of gravity for a spatially flat FRW universe. They considered a theoretical model for interacting Kaniadakis holographic dark energy with the Hubble horizon as the infrared cutoff. They dealt with two interaction scenarios between Kaniadakis holographic dark energy and matter. After studying various cosmological parameters, interestingly enough, they found that the generalized second law of thermodynamics holds for both cases of interaction terms. Moradpour et al. [77] used the first law of thermodynamics and proposed a relation between the system entropy and its IR and UV cutoffs. In addition, applying this relation to the apparent horizon of flat FRW universe, whose entropy meets the Rényi entropy, a new holographic dark energy model was addressed. Thereinafter, the evolution of the flat FRW universe, filled by a pressureless source and the obtained dark energy candidate, was studied. There is no mutual interaction between the cosmos sectors. It was found out that the obtained model is theoretically powerful to explain the current accelerated phase of the universe. This result emphasizes that the generalized entropy formalism is suitable for describing systems including long-range interactions such as gravity.

- **Jerk Parameter:** The jerk parameter is a dimensionless quantity that characterizes the third-order time derivative of the scale factor. It provides a deeper insight into the expansion dynamics of the Universe, going beyond the deceleration parameter by describing the rate at which cosmic acceleration itself is changing. This makes the jerk parameter particularly valuable for differentiating among various cosmological models, especially those involving dynamic forms of dark energy or modifications to gravity. In the standard ΛCDM model, the jerk parameter remains constant throughout the Universe's evolution. This constancy arises because ΛCDM is based on a cosmological constant with an unchanging equation of state. As a result, the expansion history follows a fixed trajectory that leads to a constant jerk value. In contrast, our model yields a present-day jerk parameter value of 0.75, which deviates from the standard value predicted by ΛCDM. This lower value suggests that the rate at which cosmic acceleration changes is more moderate in our model. While the Universe is still undergoing acceleration, the evolution of that acceleration is not as strong as it would be under the influence of a cosmological constant.A comparison of the redshift evolution of the jerk parameter, as depicted in Figure 5, shows that at early times (i.e., higher redshifts), both our model and ΛCDM display similar behavior due to the dominance of matter. However, at lower redshifts, where dark energy effects become significant, our model reveals a time-dependent jerk parameter, in contrast to the constant value in ΛCDM. This dynamical behavior allows our model to capture more complex features of the Universe's expansion, such as a possible transition in the acceleration regime or evolving properties of dark energy. The deviation of the present jerk parameter from unity highlights the capability of our model to accommodate richer cosmological dynamics. A value less than one may imply that the acceleration of the Universe could slow down in the future or that the current acceleration is driven by a mechanism other than a pure cosmological constant.In conclusion, the behavior of the jerk parameter in our model provides an effective diagnostic for distinguishing it from the ΛCDM framework. The present value of 0.75 reflects a more nuanced evolution of cosmic

 doi:10.20944/preprints202602.0082.v1

acceleration, thereby offering an alternative perspective on the nature of dark energy and the expansion history of the Universe.

- **Snap parameter :**The snap parameter is a higher-order cosmographic quantity that characterizes the fourth derivative of the scale factor with respect to cosmic time. It provides important insights into the time evolution of the jerk parameter and offers an even finer probe of the Universe's expansion history. The inclusion of the snap parameter is particularly relevant for distinguishing between subtle dynamical effects that may not be captured by the Hubble, deceleration, or jerk parameters alone. In the standard ΛCDM cosmological model, the snap parameter is constant and typically positive, consistent with a Universe governed by a cosmological constant. This constant value reflects the simplicity and fixed nature of the ΛCDM framework, in which dark energy does not evolve with time. In our model, the present-day value of the snap parameter is found to be negative, with $s_0 = -0.65$. This significant deviation from the ΛCDM value indicates a more complex expansion history. A negative snap parameter suggests that the rate of change of the jerk parameter is decreasing, which could point toward a slowdown in the acceleration or a dynamic dark energy component that evolves over time. The comparison, as shown in Figure 6, illustrates that at higher redshifts both models tend to converge due to the dominance of matter and radiation. However, in the low-redshift regime where dark energy becomes significant, our model exhibits a non-trivial evolution of the snap parameter. This dynamic behavior is not present in the constant snap value predicted by ΛCDM and highlights the increased flexibility of our model in capturing the late-time cosmological dynamics. The negative value of the present snap parameter may also imply that the Universe could transition to a different expansion phase in the future, such as a decelerated phase or a varying acceleration scenario. Such possibilities are not accommodated within the standard ΛCDM model and therefore make the snap parameter a crucial discriminator for alternative cosmological frameworks. In summary, the snap parameter in our model reveals richer cosmological dynamics and offers additional evidence of departure from the standard ΛCDM behavior. The negative value of $s_0 = -0.65$ emphasizes the potential for evolving dark energy or modified gravity and supports the utility of higher-order cosmographic diagnostics in understanding the full scope of the Universe's expansion history.
- **Equation of state parameter:** The equation of state parameter describes the relationship between pressure and energy density of the cosmic fluid and is central to understanding the nature of dark energy in general relativity. In the standard ΛCDM model, this parameter is fixed at minus one, representing a cosmological constant that drives the accelerated expansion of the Universe with a constant energy density over time. However, in our model, the equation of state parameter varies with redshift, reflecting a dynamical form of dark energy. At present, our model predicts a value of $\omega_0 \approx -0.83$, which lies in the quintessence regime. This suggests that the dark energy component in our model behaves like a slowly evolving field rather than a true constant. Compared to the ΛCDM scenario, our model allows for a slightly weaker negative pressure, implying a different rate of cosmic acceleration. This deviation indicates that the underlying mechanism driving the Universe's expansion might be more complex than a simple cosmological constant, potentially pointing toward evolving scalar fields or modified gravity effects, while still remaining consistent with current observational constraints.
- **Thermodynamic consistency:** Using the best-fit parameters obtained from the combined observational datasets ($q_0 = -0.48$ and $q_1 = 0.58$), the condition $q(z) \geq -1$ is satisfied over the observationally relevant range ($z \geq 0$), ensuring that the apparent horizon area remains non-decreasing, in accordance with the generalized second law of thermodynamics. Furthermore, as $z \to -1$ (the asymptotic future), the condition $dq/dz > 0$ implies that $q(z)$ approaches -1 from above, leading to a maximization of the apparent–horizon entropy consistent with a stable de Sitter state. The divergence of the parametrization $q(z) = q_0 + \frac{q_1 z}{1+z}$ exactly at $z \to -1$ lies far beyond the domain probed by current cosmological observations. Within the observationally relevant epoch, the model therefore remains thermodynamically admissible.

 doi:10.20944/preprints202602.0082.v1

8. Conclusion

In this work, we have investigated a novel cosmological model within the framework of a spatially flat FRW Universe, incorporating the contributions of dark energy (DE), dark matter (DM), and radiation. The core focus of our study was to construct a viable and flexible model of the Universe's accelerated expansion by introducing a new parametrization of the deceleration parameter $q(z)$, characterized by the parameters q_0 and q_1. This approach enables a model-independent exploration of cosmic dynamics, capturing both the early-time decelerated and the late-time accelerated phases of the Universe's evolution, without invoking a specific gravitational theory. To constrain the parameters of our model, we employed the Markov Chain Monte Carlo technique using a diverse and complementary set of observational datasets, including cosmic chronometers $H(z)$, Type Ia supernovae, and baryon acoustic oscillations. The reconstructed deceleration parameter exhibits a smooth transition from deceleration to acceleration, in agreement with current cosmological observations and suggesting deviations from the standard ΛCDM model. Moreover, the derived evolution of the jerk parameter and snap parameter points toward the possibility of cosmological dynamics beyond the canonical cosmological constant scenario. The diagnostic tool $\mathrm{Om}(z)$ was utilized to further analyze and classify the model, highlighting its distinct behavior compared to ΛCDM. We also applied information criteria to evaluate the goodness-of-fit and model selection capabilities, which confirm the effectiveness and compatibility of the proposed parametrization.

The framework developed here reproduces the observational evidence for late-time cosmic acceleration and yields important theoretical implications regarding the behavior and origin of dark energy. This work has the potential to open promising avenues for future research aimed at uncovering deeper aspects of cosmic acceleration and testing alternative theories of gravity through high-precision cosmological data. In summary, the proposed parametrized framework not only reproduces the observed cosmic acceleration with high consistency across multiple datasets, but also remains thermodynamically admissible within the observational range, ensuring compliance with the generalized second law of thermodynamics and offering a coherent physical picture of the late-time evolution of the Universe.

Funding: This research received no funding.

Data Availability Statement: No new data were created or analyzed in this study.

References

1. Riess, A.G.; et al. Observational evidence from supernovae for an accelerating universe and a cosmological constant. *Astron. J.* **1998**, *116*, 1009–1038. https://doi.org/10.1086/300499.
2. Perlmutter, S.; et al. Measurements of Omega and Lambda from 42 High-Redshift Supernovae. *Astrophys. J.* **1999**, *517*, 565–586. https://doi.org/10.1086/307221.
3. Spergel, D.N.; et al. First-Year Wilkinson Microwave Anisotropy Probe (WMAP) Observations: Determination of Cosmological Parameters. *Astrophys. J. Suppl. Ser.* **2003**, *148*, 175–194. https://doi.org/10.1086/377226.
4. Nojiri, S.; Odintsov, S.D. Unified cosmic history in modified gravity: from F(R) theory to Lorentz non-invariant models. *Phys. Rept.* **2011**, *505*, 59–144. https://doi.org/10.1016/j.physrep.2011.04.001.
5. Clifton, T.; Ferreira, P.G.; Padilla, A.; Skordis, C. Modified gravity and cosmology. *Phys. Rept.* **2012**, *513*, 1–189. https://doi.org/10.1016/j.physrep.2012.01.001.
6. Peebles, P.J.E.; Ratra, B. The cosmological constant and dark energy. *Rev. Mod. Phys.* **2003**, *75*, 559–606. https://doi.org/10.1103/RevModPhys.75.559.
7. Copeland, E.J.; Sami, M.; Tsujikawa, S. Dynamics of dark energy. *Int. J. Mod. Phys. D* **2006**, *15*, 1753–1936. https://doi.org/10.1142/S021827180600942X.
8. Frieman, J.A.; Turner, M.S.; Huterer, D. Dark energy and the accelerating universe. *Ann. Rev. Astron. Astrophys.* **2008**, *46*, 385–432. https://doi.org/10.1146/annurev.astro.46.060407.145243.
9. Sahni, V.; Starobinsky, A. The Case for a positive cosmological Lambda-term. *Int. J. Mod. Phys. D* **2000**, *9*, 373–443. https://doi.org/10.1142/S0218271800000542.

 doi:10.20944/preprints202602.0082.v1

10. Caldwell, R.R.; Dave, R.; Steinhardt, P.J. Cosmological imprint of an energy component with general equation of state. *Phys. Rev. Lett.* **1998**, *80*, 1582–1585. https://doi.org/10.1103/PhysRevLett.80.1582.
11. Zlatev, I.; Wang, L.; Steinhardt, P.J. Quintessence, cosmic coincidence, and the cosmological constant. *Phys. Rev. Lett.* **1999**, *82*, 896–899. https://doi.org/10.1103/PhysRevLett.82.896.
12. Padmanabhan, T. Cosmological constant: The Weight of the vacuum. *Phys. Rept.* **2003**, *380*, 235–320. https://doi.org/10.1016/S0370-1573(03)00120-0.
13. Amendola, L. Coupled quintessence. *Phys. Rev. D* **2000**, *62*, 043511. https://doi.org/10.1103/PhysRevD.62.043511.
14. Kamenshchik, A.Y.; Moschella, U.; Pasquier, V. An alternative to quintessence. *Phys. Lett. B* **2001**, *511*, 265–268. https://doi.org/10.1016/S0370-2693(01)00571-8.
15. Weinberg, S. The cosmological constant problem. *Rev. Mod. Phys.* **1989**, *61*, 1–23. https://doi.org/10.1103/RevModPhys.61.1.
16. Sahni, V. The Cosmological constant problem and quintessence. *Class. Quant. Grav.* **2002**, *19*, 3435–3448. https://doi.org/10.1088/0264-9381/19/13/304.
17. Carroll, S.M. The Cosmological constant. *Living Rev. Rel.* **2001**, *4*, 1. https://doi.org/10.12942/lrr-2001-1.
18. Padmanabhan, T. Understanding our universe: Current status and open issues. In *100 Years of Relativity: Space-Time Structure: Einstein and Beyond*; 2005; pp. 175–204, [gr-qc/0503107]. https://doi.org/10.1142/9789812700988_0007.
19. Caldwell, R.R. A phantom menace? Cosmological consequences of a dark energy component with super-negative equation of state. *Phys. Lett. B* **2002**, *545*, 23–29. https://doi.org/10.1016/S0370-2693(02)02589-3.
20. Nojiri, S.; Odintsov, S.D. Quantum de Sitter cosmology and phantom matter. *Phys. Lett. B* **2003**, *562*, 147–152. https://doi.org/10.1016/S0370-2693(03)00594-X.
21. Armendariz-Picon, C.; Mukhanov, V.; Steinhardt, P.J. A dynamical solution to the problem of a small cosmological constant and late-time cosmic acceleration. *Phys. Rev. Lett.* **2000**, *85*, 4438–4441. https://doi.org/10.1103/PhysRevLett.85.4438.
22. Sen, A. Tachyon matter. *JHEP* **2002**, *2002*, 065. https://doi.org/10.1088/1126-6708/2002/07/065.
23. Chevallier, M.; Polarski, D. Accelerating universes with scaling dark matter. *Int. J. Mod. Phys. D* **2001**, *10*, 213–223. https://doi.org/10.1142/S0218271801000822.
24. Linder, E.V. Exploring the expansion history of the universe. *Phys. Rev. Lett.* **2003**, *90*, 091301. https://doi.org/10.1103/PhysRevLett.90.091301.
25. Jassal, H.K.; Bagla, J.S.; Padmanabhan, T. Observational constraints on low redshift evolution of dark energy: How consistent are different observations? *Phys. Rev. D* **2005**, *72*, 103503. https://doi.org/10.1103/PhysRevD.72.103503.
26. Barboza, E.M.; Alcaniz, J.S. A parametric model for dark energy. *Phys. Lett. B* **2008**, *666*, 415–419. https://doi.org/10.1016/j.physletb.2008.08.012.
27. Naik, D.M.; Kavya, N.S.; Sudharani, L.; et al.. Impact of a newly parametrized deceleration parameter on the accelerating universe and the reconstruction of f(Q) non-metric gravity models. *Eur. Phys. J. C* **2023**, *83*, 840. https://doi.org/10.1140/epjc/s10052-023-12029-1.
28. Cunha, J.V.; Lima, J.A.S. Transition redshift: new kinematic constraints from supernovae. *Mon. Not. R. Astron. Soc.* **2008**, *390*, 210–217. https://doi.org/10.1111/j.1365-2966.2008.13640.x.
29. Chaudhary, H.; Mumtaz, S.; Bouali, A.; et al.. Parametrization of the deceleration parameter in a flat FLRW universe: constraints and comparative analysis with the ΛCDM paradigm. *Gen. Relativ. Gravit.* **2023**, *55*, 133. https://doi.org/10.1007/s10714-023-03181-w.
30. Akarsu, Ö.; Dereli, T. Cosmological Models with Linearly Varying Deceleration Parameter. *Int. J. Theor. Phys.* **2012**, *51*, 612–621. https://doi.org/10.1007/s10773-011-0941-5.
31. Mamon, A.A.; Das, S. A parametric reconstruction of the deceleration parameter. *Eur. Phys. J. C* **2017**, *77*, 495. https://doi.org/10.1140/epjc/s10052-017-5066-4.
32. Singh, K.P.; Sabanam, S.; Yadav, A.K.; Meitei, A.J. Modeling through the cubic parametrization of the deceleration parameter in f(R,Lm) gravity with observational constraints. *Nucl. Phys. B* **2025**, *1018*, 117061. https://doi.org/10.1016/j.nuclphysb.2025.117061.
33. Chaudhary, H.; Bouali, A.; Debnath, U.; Roy, T.; Mustafa, G. Constraints on the parameterized deceleration parameter in FRW universe. *Phys. Scr.* **2023**, *98*, 095006. https://doi.org/10.1088/1402-4896/acea02.
34. Mamon, A.A. Constraints on a generalized deceleration parameter from cosmic chronometers. *Mod. Phys. Lett. A* **2018**, *33*, 1850056. https://doi.org/10.1142/S0217732318500566.

 doi:10.20944/preprints202602.0082.v1

35. Pavón, D.; Duran, I.; del Campo, S.; Herrera, R. Parameterizing the deceleration parameter. In Proceedings of the Proceedings of the Thirteenth Marcel Grossmann Meeting on General Relativity, 2015, pp. 1564–1566. https://doi.org/10.1142/9789814623995_0225.
36. Akarsu, O.; Kumar, S.; Myrzakulov, R.; Sami, M.; Xu, L. Cosmology with hybrid expansion law: scalar field reconstruction of cosmic history and observational constraints. *JCAP* **2014**, *01*, 022. https://doi.org/10.1088/1475-7516/2014/01/022.
37. Bishi, B.K. Variable deceleration parameter and dark energy models. *Int. J. Geom. Methods Mod. Phys.* **2016**, *13*, 1650055. https://doi.org/10.1142/S0219887816500559.
38. Farooq, O.; Ratra, B. Hubble parameter measurement constraints on the cosmological deceleration-acceleration transition redshift. *Astrophys. J. Lett.* **2013**, *766*, L7. https://doi.org/10.1088/2041-8205/766/1/L7.
39. Naik, D.M.; Kavya, N.S.; Sudharani, L.; Venkatesha, V. Model-independent cosmological insights from three newly reconstructed deceleration parameters with observational data. *Phys. Lett. B* **2023**, *844*, 138117. https://doi.org/10.1016/j.physletb.2023.138117.
40. Lewis, A.; Bridle, S. Cosmological parameters from CMB and other data: A Monte Carlo approach. *Phys. Rev. D* **2002**, *66*, 103511. https://doi.org/10.1103/PhysRevD.66.103511.
41. Gelman, A.; Rubin, D.B. Inference from Iterative Simulation Using Multiple Sequences. *Statistical Science* **1992**, *7*, 457–472. https://doi.org/10.1214/ss/1177011136.
42. Scolnic, D.M.e.a. The complete light-curve sample of spectroscopically confirmed SNe Ia from Pan-STARRS1 and cosmological constraints from the combined Pantheon sample. *Astrophys. J.* **2018**, *859*, 101. https://doi.org/10.3847/1538-4357/aab9bb.
43. Alam, S.e.a. The clustering of galaxies in the completed SDSS-III Baryon Oscillation Spectroscopic Survey: cosmological analysis of the DR12 galaxy sample. *Mon. Not. R. Astron. Soc.* **2017**, *470*, 2617–2652. https://doi.org/10.1093/mnras/stx721.
44. Callen, H.B. *Thermodynamics and an Introduction to Thermostatistics*; John Wiley & Sons, 1985.
45. Bak, D.; Rey, S.J. Cosmic holography. *Class. Quantum Grav.* **2000**, *17*, L83. https://doi.org/10.1088/0264-9381/17/15/101.
46. Cai, R.G.; Kim, S.P. First law of thermodynamics and Friedmann equations of Friedmann-Robertson-Walker universe. *J. High Energy Phys.* **2005**, *2005*, 050. https://doi.org/10.1088/1126-6708/2005/02/050.
47. Akbar, M.; Cai, R.G. Thermodynamic behavior of the Friedmann equation at the apparent horizon of the FRW universe. *Phys. Rev. D* **2007**, *75*, 084003. https://doi.org/10.1103/PhysRevD.75.084003.
48. Easson, D.A.; Frampton, P.H.; Smoot, G.F. Entropic accelerating universe. *Phys. Lett. B* **2011**, *696*, 273–277. https://doi.org/10.1016/j.physletb.2010.12.025.
49. Xu, L.; Liu, H. Constraints to deceleration parameters by recent cosmic observations. *Mod. Phys. Lett. A* **2008**, *23*, 1939–1948. https://doi.org/10.1142/S0217732308025991.
50. Foreman-Mackey, D.; Hogg, D.W.; Lang, D.; Goodman, J. emcee: The MCMC Hammer. *Publications of the Astronomical Society of the Pacific* **2013**, *125*, 306. https://doi.org/10.1086/670067.
51. Lewis, A. GetDist: a Python package for analysing Monte Carlo samples. *arXiv preprint arXiv:1910.13970* **2019**. https://doi.org/10.48550/arXiv.1910.13970.
52. Simon, J.; Verde, L.; Jimenez, R. Constraints on the redshift dependence of the dark energy potential. *Phys. Rev. D* **2005**, *71*, 123001. https://doi.org/10.1103/PhysRevD.71.123001.
53. Stern, D.e.a. Cosmic chronometers: constraining the equation of state of dark energy. I: H(z) measurements. *JCAP* **2010**, *2010*, 008. https://doi.org/10.1088/1475-7516/2010/02/008.
54. Moresco, M.e.a. Improved constraints on the expansion rate of the Universe up to z 1.1 from the spectroscopic evolution of cosmic chronometers. *JCAP* **2012**, *2012*, 006. https://doi.org/10.1088/1475-7516/2012/08/006.
55. Zhang, C.e.a. Four new observational H(z) data from luminous red galaxies in the Sloan Digital Sky Survey data release seven. *Research in Astronomy and Astrophysics* **2014**, *14*, 1221. https://doi.org/10.1088/1674-4527/14/10/002.
56. Moresco, M. Raising the bar: new constraints on the Hubble parameter with cosmic chronometers at z – 2. *Monthly Notices of the Royal Astronomical Society* **2015**, *450*, L16–L20. https://doi.org/10.1093/mnrasl/slv037.
57. Moresco, M.e.a. A 6% measurement of the Hubble parameter at $z \sim 0.45$: direct evidence of the epoch of cosmic re-acceleration. *JCAP* **2016**, *2016*, 014. https://doi.org/10.1088/1475-7516/2016/05/014.
58. Brout, D.e.a. The Pantheon+ Analysis: Cosmological Constraints. *The Astrophysical Journal* **2022**, *938*, 110. https://doi.org/10.3847/1538-4357/ac8e04.

 doi:10.20944/preprints202602.0082.v1

59. Aubourg, É.; Bailey, S.; Bautista, J.E.; Beutler, F.; Bhardwaj, V.; Bizyaev, D.; Blanton, M.; Blomqvist, M.; Bolton, A.S.; et al.. Cosmological implications of baryon acoustic oscillation measurements. *Phys. Rev. D* **2015**, *92*, 123516. https://doi.org/10.1103/PhysRevD.92.123516.
60. Cuceu, A.; Farr, J.; Lemos, P.; Font-Ribera, A. Baryon acoustic oscillations and the Hubble constant: past, present and future. *J. Cosmol. Astropart. Phys.* **2019**, *2019*, 044. https://doi.org/10.1088/1475-7516/2019/10/044.
61. Philcox, O.H.E.; Ivanov, M.M. BOSS DR12 full-shape cosmology: ΛCDM constraints from the large-scale galaxy power spectrum and bispectrum monopole. *Phys. Rev. D* **2022**, *105*, 043517. https://doi.org/10.1103/PhysRevD.105.043517.
62. Alam, S.e.a. Completed SDSS-IV extended Baryon Oscillation Spectroscopic Survey: Cosmological implications from two decades of spectroscopic surveys at the Apache Point Observatory. *Phys. Rev. D* **2021**, *103*, 083533. https://doi.org/10.1103/PhysRevD.103.083533.
63. Adame, A.G.; Aguilar, J.; Ahlen, S.; Alam, S.; Alexander, D.M.; Alvarez, M.; Alves, O.; Anand, A.; Andrade, U.; Armengaud, E.; et al. DESI 2024 VI: cosmological constraints from the measurements of baryon acoustic oscillations. *J. Cosmol. Astropart. Phys.* **2025**, *2025*, 021. https://doi.org/10.1088/1475-7516/2025/02/021.
64. Pacif, S.K.J.; Myrzakulov, R.; Myrzakul, S. Reconstruction of cosmic history from a simple parametrization of H. *International Journal of Geometric Methods in Modern Physics* **2017**, *14*, 1750111. https://doi.org/10.1142/S0219887817501110.
65. Nair, R.; Jhingan, S.; Jain, D. Cosmokinetics: a joint analysis of standard candles, rulers and cosmic clocks. *J. Cosmol. Astropart. Phys.* **2012**, *2012*, 018. https://doi.org/10.1088/1475-7516/2012/01/018.
66. Lu, J.; Xu, L.; Liu, M. Constraints on kinematic models from the latest observational data. *Phys. Lett. B* **2011**, *699*, 246–250. https://doi.org/10.1016/j.physletb.2011.04.022.
67. Mamon, A.A.; Das, S. A divergence-free parametrization of deceleration parameter for scalar field dark energy. *Int. J. Mod. Phys. D* **2016**, *25*, 1650032. https://doi.org/10.1142/S0218271816500322.
68. del Campo, S.; Duran, I.; Herrera, R.; Pavón, D. Three thermodynamically based parametrizations of the deceleration parameter. *Phys. Rev. D* **2012**, *86*, 083509. https://doi.org/10.1103/PhysRevD.86.083509.
69. Pavón, D.; Duran, I.; del Campo, S.; Herrera, R. Parameterizing the Deceleration Parameter, 2012, [arXiv:gr-qc/1212.6874].
70. Mamon, Abdulla Al.; Das, Sudipta. A parametric reconstruction of the deceleration parameter. *Eur. Phys. J. C* **2017**, *77*, 495. https://doi.org/10.1140/epjc/s10052-017-5066-4.
71. Myrzakulov, Y.; Donmez, O.; Koussour, M.; Muminov, S.; Dauletov, A.; Rayimbaev, J. Thermodynamic constraints and observational validation of the deceleration parameter. *Nuclear Physics B* **2025**, *1016*, 116916. https://doi.org/https://doi.org/10.1016/j.nuclphysb.2025.116916.
72. Azhar, N.; Rani, S.; Jawad, A.; Alam, M.M.; Shaymatov, S. Cosmic and thermodynamics consequences of Chaplygin–Jacobi corrected HDE model. *Phys. Dark Univ.* **2025**, *47*, 101819. https://doi.org/10.1016/j.dark.2025.101819.
73. Azhar, N.; Jawad, A.; Ahmed, I.; Alam, M.M.; Shaymatov, S. Cosmographic and thermodynamics analysis of five dimensional EChS gravity. *J. High Energy Astrophys.* **2025**, *47*, 100369. https://doi.org/10.1016/j.jheap.2025.100369.
74. Jawad, A.; Ahsan, A.; Rani, S. Cosmographic analysis of holographic nonzero torsion framework. *Int. J. Geom. Methods Mod. Phys.* **2024**, *21*, 2450241. https://doi.org/10.1142/S0219887824502414.
75. Jawad, A.; Azhar, N.; Rani, S.; Azhar, M.R.; Ahsan, A. Cosmic visualizations of equation of state parameterizations in mimetic cosmology. *Chin. J. Phys.* **2024**, *89*, 429–442. https://doi.org/10.1016/j.cjph.2024.02.018.
76. Sania.; Azhar, N.; Rani, S.; Jawad, A. Cosmic and thermodynamic consequences of Kaniadakis holographic dark energy in Brans–Dicke gravity. *Entropy* **2023**, *25*, 576. https://doi.org/10.3390/e25040576.
77. Moradpour, H.; Moosavi, S.A.; Lobo, I.P.; et al.. Thermodynamic approach to holographic dark energy and the Rényi entropy. *Eur. Phys. J. C* **2018**, *78*, 829. https://doi.org/10.1140/epjc/s10052-018-6309-8.